

## Hepatic Lymphoma: A Perplexing CT Diagnosis made Easy by <sup>18</sup>F-FDG PET CT Imaging

Shivalingappa Shivakumar Swamy\*, Mahesh Ashok Kumar, Avinash Kesari Rao, Indresh Desai, Sudhakar Sampangi, Yashaswini K and Nikita Jain

Radiology, Healthcare Global, Bangalore, India

\*Corresponding author: Shivalingappa Shivakumar Swamy, Sr. Consultant & Head, Radiology, Healthcare Global, Bangalore, India, E-mail: drshiv.radiologist@gmail.com

Received date: September 21, 2018; Accepted date: November 10, 2018; Published date: November 17, 2018

Copyright: ©2018 Swamy SS, et al. This is an open-access article distributed under the terms of the Creative Commons Attribution License, which permits unrestricted use, distribution, and reproduction in any medium, provided the original author and source are credited.

### Abstract

Hepatic involvement of lymphomas can be primary or secondary. Secondary involvement being more common and is commonly associated with NHL. Primary hepatic lymphoma is a term given for rare form of extranodal NHL. The diagnosis is often difficult on routine radiologic imaging as the imaging features are variable in appearance and there is considerable overlap with other hepatic masses.

Though CT and MRI is the mainstay of imaging modalities for all hepatobiliary cancers, misdiagnosis and mistreatment are frequently encountered even with best of the best radiologic imaging practices. Primary hepatic lymphomas are usually large mass forming lesions in the liver, whereas in secondary lymphomas can present with diffuse parenchymal involvement or nodules.

There are many reports of hepatectomies and segmental resections of the liver due to indeterminate imaging findings and misdiagnosis. We present a problem solving case of hepatic lymphoma stressing on CT and <sup>18</sup>F-FDG PET CT imaging. The diagnosis is made easy with FDG PET CT. After 3 cycles of CHOP regimen, a repeat and follow up PET scan revealed good response to chemotherapy.

**Keywords:** Hepatic lymphoma; Radiologic imaging; <sup>18</sup>F-FDG PET CT imaging

**Abbreviations:** AFP: Alpha Feto Protein; CEA: Carcinoembryonic Antigen; CT: Computed Tomography; DLBCL: Diffuse Large B-Cell Lymphoma; FDG: Fludeoxyglucose; HCC: Hepatocellular Carcinoma; HL: Hepatic Lymphoma; IHC: Immunohistochemistry; IPI: International Prognostic Index; LDH: Lactate Dehydrogenase; LIRAD: Liver Imaging and Reporting Data System; LR: LI-Rad Category; LR-M: Probably Malignancy, not specific to HCC; NHL: Non-Hodgkin Lymphoma; PET CT: Positron Emission Tomography-Computed Tomography; PHL: Primaryhepatic Lymphoma; SGPT (ALT): Serum Glutamate-Pyruvate Transaminase (Alanine Transaminase); SGOT (AST): Serum Glutamic Oxaloacetic Transaminase (Aspartate Transaminase); SUV: Standardized Uptake Value

### Case Report

A 71-years-old male, presented with history of fever of 2 months duration, right upper quadrant pain and subjective weight loss of approximately 8-9 kgs in two months.

He was evaluated with abdominal sonography followed by CT abdomen, which revealed space occupying necrotic lesion in liver of 11 cm size in the background of fatty infiltration.

The initial contrast enhanced CT revealed solitary thick walled necrotic lesion. He was treated for amoebic liver abscess with sendazole as amoebic liver disease is rampant in Indian scenario.

This was followed by antibioticsemperically for probable urinary tract infection. There was no significant improvement.

Follow up ultrasound abdomen after one month revealed the increasing size of the lesion and an interval appearance of satellite nodule.

Further liver cytology was undertaken and was reported as high-grade malignant tumor, probably sarcoma or carcinoma.

He was later investigated for metastatic versus primary liver malignancy. His blood investigations are as follows:

The screening for HBSAg, HCV and HIV sero markers were non-reactive. The AFP levels were <1.3 ng/mL and CEA <0.5 ng/mL.

Haemoglobin: 10.9 gm/dl, Total Count: 6.06 x 10<sup>9</sup> /L, Platelet Count: 327 x 10<sup>3</sup>/UL, Neutrophils: 76.4%, Lymphocytes: 16.0%, Monocytes: 7.0%, Eosinophils: 0.4%, Basophils: 0.2%; GGT: 325 U/L, Total Proteins: 6.0 g/dL.

Albumin: 2.3 g/dL, Globulin: 3.7 g /dL, A/G Ration: 0.6, SGPT (ALT): 75 U/L, SGOT (AST): 119 U/L, Alkaline Phosphatase: 411 U/L, Total Bilirubin: 0.74 mg / dL, Conjugated Bilirubin: 0.45 mg/dL; Blood Urea Nitrogen: 14 mg/dL, Creatinine: 0.8 mg/dL; Uric acid: 4.3 mg/dL; Serum Calcium: 7.4 mg/dL; Phosphorous: 3.0 mg/dL; Potassium: 4.1 mmol/L; LDH: 1458 U/L.

### Imaging

The patient was further evaluated with PETCT.6.0 millicuries of <sup>18</sup>F-fluorodeoxyglucose (FDG) was injected intravenously and after 60 min of uptake time.

He underwent whole body scan in a dedicated PET/CT scanner. The fasting blood glucose was 97 mg/dl at the time of scan.

CT component of the PETCT was performed with triple-phase contrast scan in the same setting. We applied LI-RAD for characterization of the mass on CT imaging.

The mass was well-defined and showed relative peripheral hypervascular areas in the arterial phase (Figure 1).



**Figure 1:** (a) Axial CT upper abdomen at the level of Liver in arterial phase-Poorly marginated peripheral hyper enhancing mass seen (arrows). The maximum attenuation of the lesion is HU-113; The maximum attenuation of the normal appearing liver parenchyma is HU-107. Portal (b), venous (c) and delayed (d) contrast CT images of the liver. The mass remains hypoenhancing to the liver parenchyma. No obvious capsular enhancement seen. Irregular areas of central necrosis is also seen. Note the opacified and splayed intrahepatic right and left portal veins. The maximum attenuation value of the solid portion of the mass lesion remained HU-109 in portal and venous phases. Where as the attenuation of the normal liver parenchyma were HU-155 and HU-133 respectively. On delayed scans (10 mins post IV contrast injection), the attenuation values of lesion is HU-88 and the normal appearing liver parenchyma is HU-105.

It was hypoenhancing compared to the rest of the normal liver parenchyma in the portal, venous and delayed phases (Figure 1). No delayed capsular enhancement seen.

The portal veins were splayed without thrombus. The hepatic veins and IVC were normal. There was a definite increase in the size of the mass.

At this stage, based on CT images, the mass was categorized as LR - M and/or LR4 of LI-RAD category.

This was based on 10%-29% arterial hyper enhancement and a threshold increase in size of approximately two times. The <sup>18</sup>F-FDG PET CT revealed peripherally FDG avid hepatic lesions. The maximum SUV of the hepatic lesions was 41.4 (Mean SUV 27.8) (Figure 2).

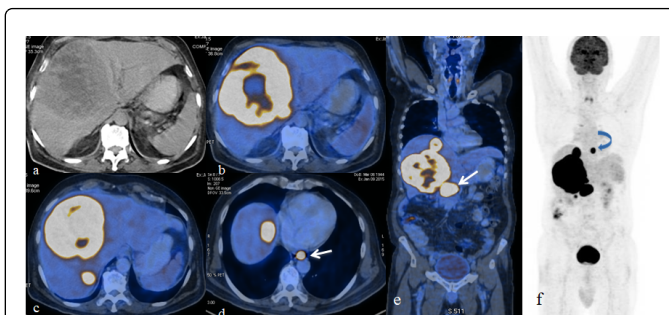


**Figure 2:** Axial CT (a) and PETCT (b-d) axial fusion images of the liver; predominantly peripheral intense FDG activity seen in the hepatic lesions. Note lower posterior mediastinal lymph node in Figure 2d (arrow). Coronal PETCT fused (e) and maximum intensity projection (f) PET images. Shows intense metabolically active hepatic masses with portocaval (arrow) and lower posterior mediastinal lymph nodes (curved arrow).

There were also PET avid portocaval and lower posterior mediastinal lymph nodes with maximum SUV of 49.0 (Figure 2).

The tumor had doubled in size over a span of 60 days and there were additional small new lesions in segment VII and VIII of the liver (Figures 3a and 3b).

A repeat ultrasound guided liver biopsy was performed based on the PET CT and biochemical reports. The biopsy revealed B cell NHL DLBCL CD 20+ disease (Figures 3c and 3d).

The bone marrow aspiration did not reveal lymphomatous involvement of the marrow. Bone marrow biopsy however revealed hypercellular marrow with nodular lymphomatous involvement. The IPI score was of 4.

### Immunohistochemistry

Immunohistochemistry shows that the neoplastic cells express CD20, CD10 and negative for CD3. Ki-67 proliferation index was 50%. Cytogenetics was normal (Figures 3e-3g).

He was vaccinated with Pneumovax, Meningococcal, Hiberax. The patient received three cycles of R-CHOP (Rituximab, Vincristine, Adriamycin, Endoxan, Prednisolone) regimen at 80% dose. He underwent assessment <sup>18</sup>F-FDG PET CT after three cycles of chemotherapy.

The study revealed significant regression in size and enhancement of the hepatic lesions (Figures 3h and 3i). The portocaval and lower posterior mediastinal lymph nodes also showed significant regression.

<sup>18</sup>F-FDG PETCT revealed significant regression in SUV of hepatic lesions (SUV 4.13) with resolution of metabolic activity in the portocaval and lower posterior mediastinal lymph nodes (Figures 3j and 3k).

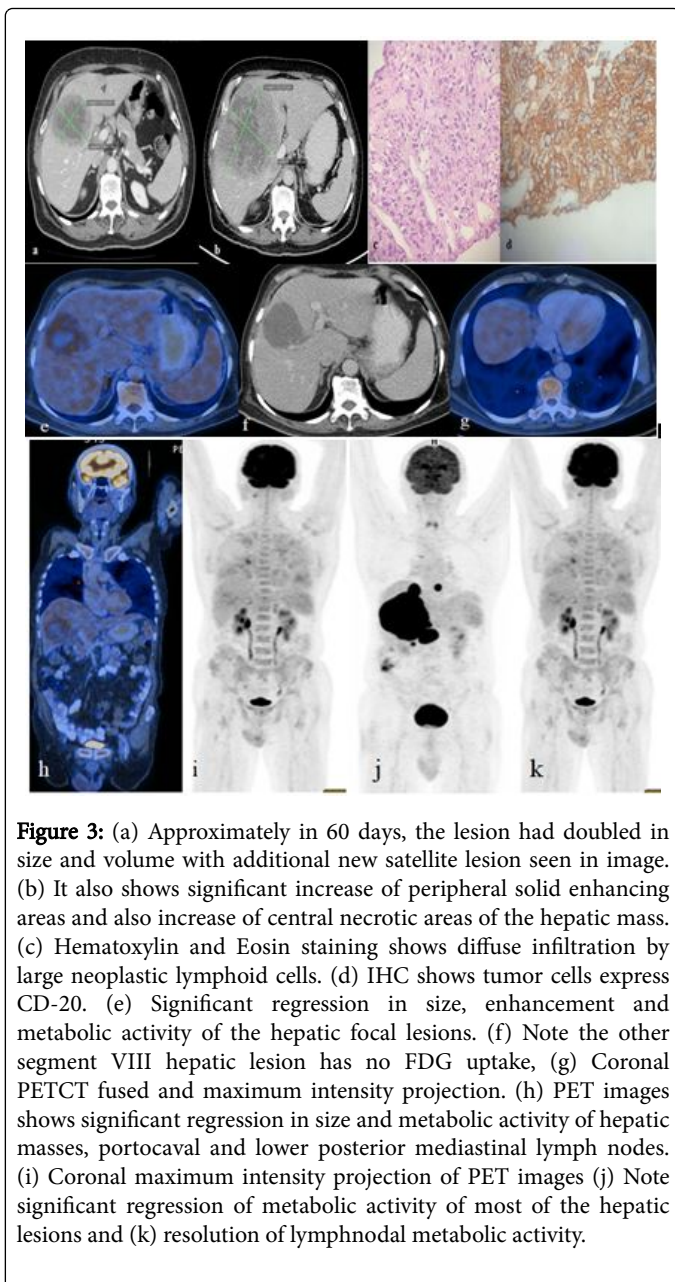


**Figure 3:** (a) Approximately in 60 days, the lesion had doubled in size and volume with additional new satellite lesion seen in image. (b) It also shows significant increase of peripheral solid enhancing areas and also increase of central necrotic areas of the hepatic mass. (c) Hematoxylin and Eosin staining shows diffuse infiltration by large neoplastic lymphoid cells. (d) IHC shows tumor cells express CD-20. (e) Significant regression in size, enhancement and metabolic activity of the hepatic focal lesions. (f) Note the other segment VIII hepatic lesion has no FDG uptake, (g) Coronal PETCT fused and maximum intensity projection. (h) PET images shows significant regression in size and metabolic activity of hepatic masses, portocaval and lower posterior mediastinal lymph nodes. (i) Coronal maximum intensity projection of PET images (j) Note significant regression of metabolic activity of most of the hepatic lesions and (k) resolution of lymphnodal metabolic activity.

## Discussion

PHL is a rare form of extranodal lymphomas, accounting for less than 1% of all extranodal lymphomas [1]. PHL is defined as lymphoma that is confined to the liver and perihepatic lymph nodes, without evidence of involvement of other visceral organs, distant lymph nodes or bone marrow for at least 6-months after the onset of hepatic disease [2].

Secondary hepatic involvement by lymphoma is relatively common and occurs in up to 50% of patients with non-Hodgkin lymphoma and in around 20% of patients with Hodgkin disease [3,4]. Etiologic factors implicated to be associated are Epstein-Barr virus (EBV) prior infection, hepatitis B and C (HBV, HCV), and cirrhosis [5]. Our patient was non-reactive for all the above viral markers.

Right upper quadrant abdominal pain, hepatomegaly, and palpable liver are the main presenting features. Jaundice and hepatic failure are also reported [6]. Yet, most of the time, the diagnosis is an incidental finding, during evaluation for nonspecific symptoms as nausea, mild abdominal discomfort, or early satiety, as in our case. The hepatic involvement may have a nodular or diffuse pattern and has got no actual prognostic value [7].

Most HLs are diffuse large B-cell lymphomas (DLBCL), while T-cell PHL are reported very infrequently. Other histologic subtypes include high-grade tumors (lymphoblastic and Burkett lymphoma, 17%), follicular lymphoma (4%), lymphoma of the mucosa-associated lymphoid tissue type, anaplastic large-cell lymphoma, mantle cell lymphoma, T-cell-rich B-cell lymphoma, and hepatosplenic T-cell lymphoma [8].

On laboratory data, alkaline phosphatase (ALP) and lactic dehydrogenase (LDH) are elevated most of the time, while tumor markers as  $\alpha$ -fetoprotein (AFP) and carcinoembryonic antigen (CEA) remain between normal ranges. Tumor markers help in differential diagnosis from hepatocellular carcinoma or metastatic disease.

Triple phase dynamic contrast enhanced CT imaging is standard imaging technique in assessing the hepatic masses and in particular HCC. CT and/or MRI are utilized in noninvasive diagnosis of HCC. To improve standardization and consensus in interpreting and reporting CT and MRI examinations of the liver in patients at risk for HCC, LI-RADS was launched in March 2011 and adopted for the diagnosis of HCC.

This method of categorizing liver findings for patients with cirrhosis or other risk factors for developing HCC allows the radiology community to apply consistent terminology, reduce imaging interpretation variability and errors, enhance communication with referring clinicians and facilitate quality assurance and research [9].

Based on the triple phase contrast CT imaging, the tumor was categorized as LR-M and/or LR4 of LI-RAD category [9]. CT imaging of hepatic lymphomas vary depending on primary or secondary involvement. On CT, hepatic lymphomas typically presents as a hypoattenuating lesion. A central area of low attenuation area indicating necrosis may be present.

Enhancement patterns on dynamic or triple phase contrast imaging are quite variable; 50% of HL lesions do not enhance at all, 33% show patchy enhancement, and 16% show ring enhancement [10].

<sup>18</sup>F FDG PET CT has been utilized in initial assessment of HCC, treatment response, intrahepatic recurrences and extrahepatic metastases in one go. Studies have shown that there are variety of different levels of glucose-6-phosphatase activity and glucose transporters in HCC, leading to variable <sup>18</sup>F-FDG uptake [11-14].

Torizuka et al. [11] showed that FDG uptake of HCC lesions correlates with the degree of differentiation of the HCC; high-grade HCCs have increased FDG uptake (+mean [ $\pm$  SD] standardized uptake value [SUV], 6.89  $\pm$  3.39) compared with low-grade HCCs (mean SUV, 3.21  $\pm$  0.58) ( $p < 0.005$ ). The maximum SUV of the hepatic lesions in our case was 41.4 (Mean SUV 27.8).

FDG PET CT is strongly recommended before treatment for patients with routinely FDG-avid, potentially curable lymphomas to better delineate the extent of disease [15]. Pretreatment PET staging of lymphomas determines the extent of disease and helps direct therapy [16] and most studies have shown high sensitivity in lymphoma

staging. In contrast to HCC, hepatic lymphomas show very high FDG avidity on PETCT.

Gota et al. [17] showed that in primary Hodgkin's disease of the liver showed maximum SUV of 21.9 in the hepatic lesions. The maximum SUV of the hepatic lesions in our case was 41.4 (Mean SUV 27.8) and the portocaval lymphnodes documented high SUV of 49.0.

The SUV documented was considerably high compared to high grade HCC by Torizuka et al. [11] or even in primary hepatic Hodgkin's disease by Gota et al. [17] Post three cycles of chemotherapy with R-CHOP regimen, the maximum SUV of the hepatic lesions dropped significantly to 4.13.

## Conclusion

<sup>18</sup>F FDG PET CT is now accepted modality of imaging in lymphomas and also in the treatment response evaluation. PHL is a rare form of NHL often faced with diagnostic challenges. The high SUV values in hepatic masses on <sup>18</sup>F FDG PET CT are very useful in attaining the diagnosis of lymphomas. A guided percutaneous biopsy either by CT or ultrasound from the most PET avid regions is crucial. This can significantly bring down the incidence of hepatic resections and surgical morbidity.

This can also minimize the incidence of repeat biopsies as the pathologists face challenges due to lot of tissue necrosis in large masses. Though strict adherence to predefined reconstruction algorithms and timing of PET imaging after FDG injection is mandatory in PET imaging for measurements of the SUV; nevertheless, primary hepatic lymphomas show intense PET avidity and differentiation between HCC is possible based on the SUV values.

We conclude that hepatic lymphomas show very high SUV compared to other primary malignant lesions of the liver. Large randomized studies are required for the establishment of the same.

## References

1. Ryan J, Straus DJ, Lange C (1988) Primary lymphoma of the liver. *Cancer* 61: 370-375.
2. Lei KI (1998) Primary non-Hodgkin's lymphoma of the liver. *Leuk Lymphoma* 29: 293-299.
3. Page RD, Romaguera JE, Osborne B, Medeiros LJ, Rodriguez J, et al (2001) Primary hepatic lymphoma: Favorable outcome after combination chemotherapy. *Cancer* 92: 2023-2029.
4. Freeman C, Berg JW, Cutler SJ (1972) Occurrence and prognosis of extranodal lymphomas. *Cancer* 29: 252-260.
5. Salmon JS, Thompson MA, Arildsen RC, Greer JP (2006) Non-Hodgkin's lymphoma involving the liver: Clinical and therapeutic considerations. *Clin Lymph and Myelo* 6: 273-280.
6. Anthony PP, Sarsfield P, Clarke T (1990) Primary lymphoma of the liver: Clinical and pathological features of 10 patients. *J Clin Pathol* 43: 1007-1013.
7. Levin NA, Berger I, Shtalrid M, Schlanger H, Sthoeger ZM (2004) Primary hepatic lymphoma: A case report and review of the literature. *Age and Ageing* 33: 637-640.
8. Masood A, Kairouz S, Hudhud KH, Hegazi AZ, Banu A et al. (2009) Primary non-Hodgkin lymphoma of liver. *Current Oncology* 16: 74-77.
9. Liver Imaging Reporting and DataSystem. American College of Radiology.
10. Blechacz B, Gores GJ (2010) PET scan for a hepatic mass. *Hepatology* 52: 2186-2191.
11. Torizuka T, Tamaki N, Inokuma T (1995) In vivo assessment of glucose metabolism in hepatocellular carcinoma with FDG-PET. *J Nucl Med* 36: 1811-1817.
12. Salem N, MacLennan GT, Kuang Y (2007) Quantitative evaluation of 2-deoxy-2 [F-18] fluoro-D-glucose-positron emission tomography imaging on the woodchuck model of hepatocellular carcinoma with histological correlation. *Mol Imaging Biol* 9: 135-143.
13. Lee JD, Yang WI, Park YN (2005) Different glucose uptake and glycolytic mechanisms between hepatocellular carcinoma and intrahepatic mass-forming cholangiocarcinoma with increased (18) F-FDG uptake. *J Nucl Med* 46: 1753-1759.
14. Roh MS, Jeong JS, Kim YH, Kim MC, Hong SH (2004) Diagnostic utility of GLUT1 in the differential diagnosis of liver carcinomas. *Hepatogastroenterology* 51: 1315-1318.
15. ChesonBD, Pfistner B, Juweid ME (2007) Revised response criteria for malignant lymphoma. *J ClinOncol* 25: 579-586.
16. Cheson BD (2011) Role of functional imaging in the management of lymphoma. *J ClinOncol* 29: 1844-1854.
17. Gota VS, Purandare NC, Gujral S, Shah S, Nair R, et al. (2009) Positron emission tomography/computerized tomography evaluation of primary Hodgkin's disease of liver. *Indian J Cancer* 46: 237-239.